PAPER

Comparison of discharge characteristics and methylene blue degradation through a direct-current excited plasma jet with air and oxygen used as working gases

Comparison of discharge characteristics and methylene blue degradation through a direct-current excited plasma jet with air and oxygen used as working gases

Jiacun WU (武珈存)**, Kaiyue WU** (吴凯玥)**, Chenhua REN** (任晨华)**,
Pengying JIA** (贾鹏英) **and Xuechen LI** (李雪辰)

College of Physics Science and Technology, Hebei University, Baoding 071002, People's Republic of China

E-mail: plasmalab@126.com

CrossMark

Abstract

Through using a direct-current driven plasma jet operated underwater, degradation of methylene blue (MB) is investigated with air and oxygen used as working gases. With a low power voltage, a plasma plume extends from the needle electrode, which is purple in air. It turns pink after it bridges the two electrodes. During the process, oxygen plasma remains white. Discharge operates in a pulsed mode or a continuous one, which depends on the magnitude of power voltage. For the pulsed mode, oxygen discharge has a shorter plume and a higher pulse frequency than air discharge under the same power voltage. For the same current of the continuous mode, both power and gap voltages of oxygen discharge are higher than those of air discharge. Moreover, MB degradation efficiency increases with increasing power voltage or initial concentration of MB solution. Compared with air discharge, oxygen discharge has a higher degradation efficiency with the same power voltage and treatment time. The pulsed oxygen discharge with power voltage of about 6.5 kV has the highest efficiency in degrading MB dye, reaching approximately 85.8% after 10 min treatment. As a comparison, after 10 min treatment in air discharge, the highest degradation efficiency is 63.7%, which appears in the continuous mode at a power voltage of 10.6 kV. Besides, optical spectra from the discharges are also compared for the two types of working gases.

(Some figures may appear in colour only in the online journal)

1. Introduction

Dyes can hardly be degraded effectively by traditional physical technologies, such as adsorption, coagulation, and filtration. The emission of not fully treated dye wastewater has become a threat to environmental protection [1, 2]. In order to effectively degrade dyes, advanced oxidation techniques have been proposed, which include ultraviolet photolysis [3], photo-catalysis [4], Fenton process [5], and gas discharge plasma technology [6–8]. Compared with its counterparts, plasma technology can effectively degrade organic dyes as a low-cost method because plasma generated by gas discharge is abundant with chemically active species [9, 10].

Dye degradation has been investigated in discharges with various working gases [11–14]. A pulsed corona discharge in air is generated above liquid surface by dual pins, and a degradation efficiency of about 96% is achieved for initial concentration of $10 \, \text{mg} \, \text{l}^{-1}$ acid blue 25 after 35 min treatment [12]. With air and oxygen used as working gases, a double-chamber dielectric barrier discharge (DBD) is used to decompose MB dye ($100 \, \text{mg} \, \text{l}^{-1}$), reaching a degradation efficiency of 99.98% after 20 min treatment by oxygen
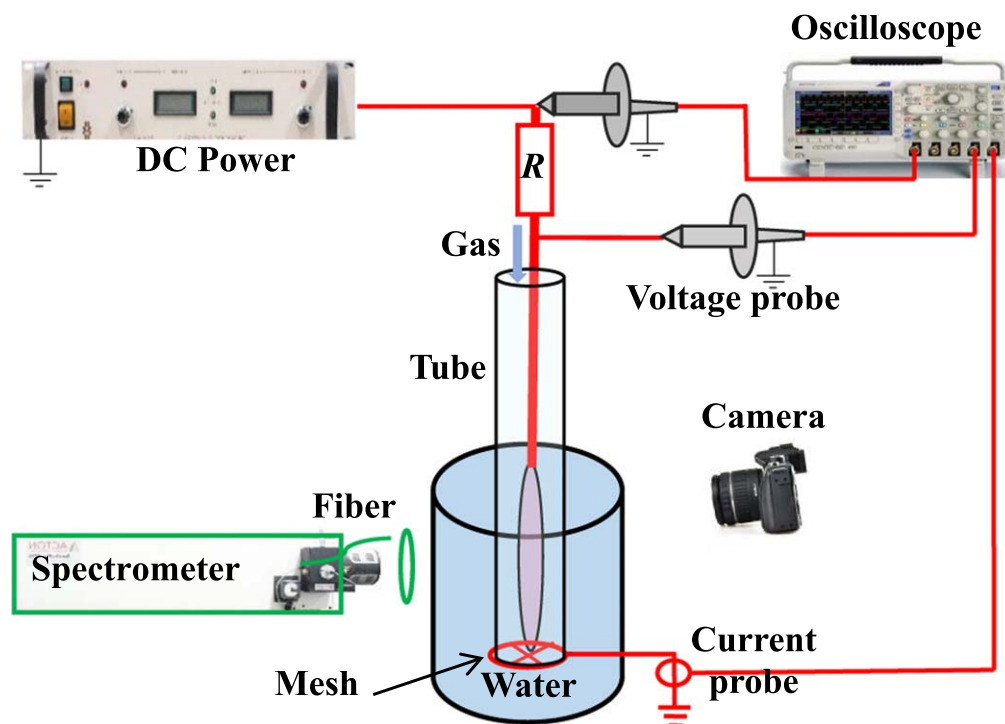
Figure 1. Schematic diagram of the experimental setup.

plasma, while only 85.3% after 100 min treatment by air plasma [13]. With nitrogen, neon, argon, and oxygen used as working gases, degradation efficiency of acid red B dye $(100 \, \mathrm{mg \, l^{-1}})$ after 10 min treatment by an abnormal glow discharge reaches 97%, 70%, 60%, and 50%, respectively [14]. Apparently, the component of working gas has a great influence on degradation efficiency of organic dyes. It is worth noting that all the aforementioned plasmas are produced above the liquid surface. Compared with them, underwater discharge has an improved reaction rate due to reactive species directly penetrating into liquid from bubbles [15]. Employing underwater oxygen plasma excited by nanosecond pulses, a high degradation efficiency of 97% is achieved after 30 min treatment of MB dye $(50 \, \mathrm{mg \, l^{-1}})$. In our previous work, degradation of MB dye has been investigated using an underwater air plasma jet excited by a direct-current (DC) voltage [16].

In this paper, MB dye degradation are compared through using the underwater DC plasma jet with air and oxygen used as working gases, respectively. Optical and electrical aspects as well as emission spectrum are compared for the discharges in the two different gases.

2. Experimental setup

Figure 1 presents a schematic diagram of the experimental setup. The plasma jet is the same as that used in [14]. A tungsten needle with a tip radius of about 200 μm has a diameter of 1.0 mm, which is coaxially placed in a tube with 8.0 mm inner diameter. The mesh electrode is mounted on the tube end, which is 1.0 cm away from the needle tip. Working

gas, air or oxygen (a purity of 99.99%), flows along the tube, whose flow rate (Q) is regulated by a flowmeter. The needle is electrically connected to the output of a DC power supply (Glassman EK15R40) via a shunt resistor (500 kΩ), and the mesh electrode is grounded. Two voltage probes (Tektronix P6015A) and a current probe (Tektronix TCPA300) are utilized to detect power voltage, gap voltage and discharge current, which can be simultaneously recorded by an oscilloscope (Tektronix DPO4104). Here, gap voltage is detected between the needle electrode and the ground electrode by one high-voltage probe, the other probe is used to detect power voltage between the power supply output and the ground electrode. A digital camera (Canon EOS7D) is used to capture discharge images with an exposure time of 1.0 s. A spectrometer (ACTON SP2750) equipped with a charge-coupled device (CCD) (PI PIXIS) is utilized to collect optical emission spectrum with a CCD exposure time of 0.5 s.

MB solution is chosen as an indicator to evaluate chemical reactivity of the underwater jet, which is filled in a 50 ml beaker maintained at a constant temperature of about 35 °C through cooling the beaker by water circulation. The plasma jet is immersed in the solution with the mesh placed 4.0 mm above the beaker bottom. Moreover, an UV–vis-NIR spectrophotometer (Perkin Elmer, Lambda 950) is used to measure absorbance of MB solution at 664 nm. Degradation efficiency of MB $(D\%)$ is calculated by the following formula.

$$D\% = (A_0 - A_t)/A_0 \times 100\%. \tag{1}$$

Here A_0 and A_t are the optical absorbance of MB solution before and after treatment, respectively.
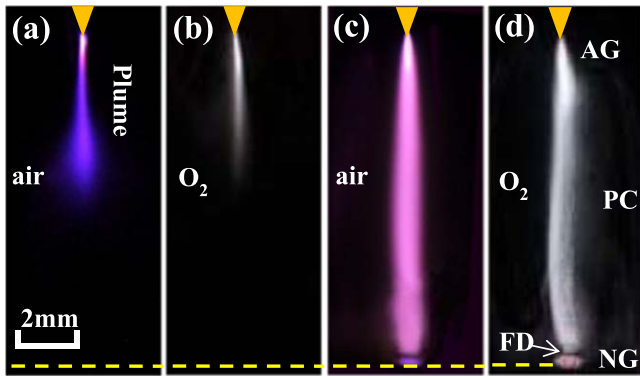
Figure 2. Images of air and oxygen discharges under different power voltages. (a) and (b) 5.0 kV, (c) and (d) 7.7 kV. Gas flow rate is $0.4\,l\,min^{-1}$, and exposure time is 1.0 s. The triangle and the dashed line denote the needle and the mesh electrode, respectively.

3. Experimental results and discussion

Figure 2 presents discharge images with oxygen and air used as the working gas, respectively. A purple plasma plume in air extends from the needle tip under a low power voltage, as shown in figure 2(a). However, it is white in oxygen (figure 2(b)), which is slightly slimmer than that in air. With increasing power voltage, plasma can bridge the two electrodes, as shown in figures 2(c) and (d). The bridging plasma is pink in air, while still white in oxygen. Furthermore, the bridging plasma has characteristic regions of low-pressure glow discharge, such as a negative glow (NG), a Faraday dark space (FD), a positive column (PC), and an anode glow (AG). The existence of these characteristic regions verifies that the bridging plasma is in a glow discharge regime.

Figure 3 presents waveforms of power voltage, gap voltage and discharge current for the discharges in figure 2. Under a low power voltage, both discharge current and gap voltage oscillates periodically, while power voltage keeps constant. Hence, the plasma jet before bridging the two electrodes operates in a pulsed mode. Due to electronegative nature, electrons can be easily attached by oxygen molecules. Therefore, compared with oxygen discharge, air discharge has a higher electron density due to its lower oxygen content. Denser electrons usually lead to a high current. Consequently, averaged current amplitude of air discharge is higher than that of oxygen discharge in the pulsed mode. Compared with the pulsed mode, both voltage and current keep invariant with time under high power voltage. The invariant current implies that the discharge is in a steady state (a continuous mode). Therefore, the discharge with low power voltages operates in the pulsed mode, which transits to the continuous mode with high power voltage.

The grey level of discharge images is higher in plume than the background, which is lower than a certain value at plume end. Through this method, plume length can be directly determined from plume images, which is presented as a function of power voltage in figure 4(a). Plume length increases with increasing power voltage until it suddenly reaches the maximal value of 10 mm, which is determined by the electrode separation. Before that, air plume is longer than oxygen plume under the same power voltage.

Spatial distribution of the applied electric field is not uniform for the plasma jet, which has a maximum at the needle tip, and decreases along the gas stream. Therefore, discharge firstly initiates in the vicinity of the needle tip, and a positive streamer extends along the gas flow [17]. Let us suppose that the streamer cannot be maintained at positions farther than a critical position due to the decreasing field intensity. Thus, the critical position determines the plume length. Compared with oxygen discharge, critical position of air discharge is farther because breakdown threshold of air is lower than that of oxygen. Consequently, for the pulsed mode, air discharge has a longer plume than oxygen discharge with the same power voltage. Moreover, an increment in power voltage leads to increased field intensity at every position. Accordingly, the critical position advances towards the mesh. As a result, plume length increases with increasing power voltage until the plasma bridges the two electrodes.

From figure 3, dissipated power (P) can be calculated from discharge current [$I(t)$] and gap voltage [$U(t)$] by the following equation.

$$P = \frac{1}{T} \int_{t}^{t+T} I(t) \times U(t)\mathrm{d}t. \tag{2}$$

Here, T denotes voltage period. Then, P is investigated as a function of power voltage, as presented in figure 4(b). Obviously, the pulsed mode dissipates a much lower power than the continuous mode. Moreover, the dissipated power of oxygen discharge is higher than that of air discharge under the same power voltage.

For the pulsed mode, discharge frequency is investigated as a function of power voltage. As shown in figure 5(a), pulse frequency increases with increasing power voltage for the discharge in air or oxygen. Moreover, oxygen discharge has a higher pulse frequency than air discharge. As mentioned above, a positive streamer mechanism is involved in the pulsed mode. After the quenching of one streamer, positive ions left in the streamer head continue to drift towards the mesh. The electric field will recover and the next discharge will initiate after these ions enter the mesh. Therefore, the drifting velocity of positive ions, which is positively correlated with field intensity, determines the time interval between discharges, which is reciprocal of pulse frequency. Besides, the distance from the mesh to the plume end, where positive ions are accumulated, influences discharge frequency. Obviously, discharge frequency will increase with increasing field intensity or plume length. As mentioned before, both field intensity and plume length increase with increasing power voltage, leading to the increasing pulse frequency with power voltage. On one hand, the field threshold for streamer quenching in oxygen is higher than that in air. Hence, positive ions in oxygen drift in a stronger field than those in air, which leads to a higher pulse frequency in oxygen. On the other hand, air plume is longer than oxygen plume, which makes a higher frequency in air. Under the competing effects of the two factors, oxygen discharge has a higher pulse frequency than air discharge.
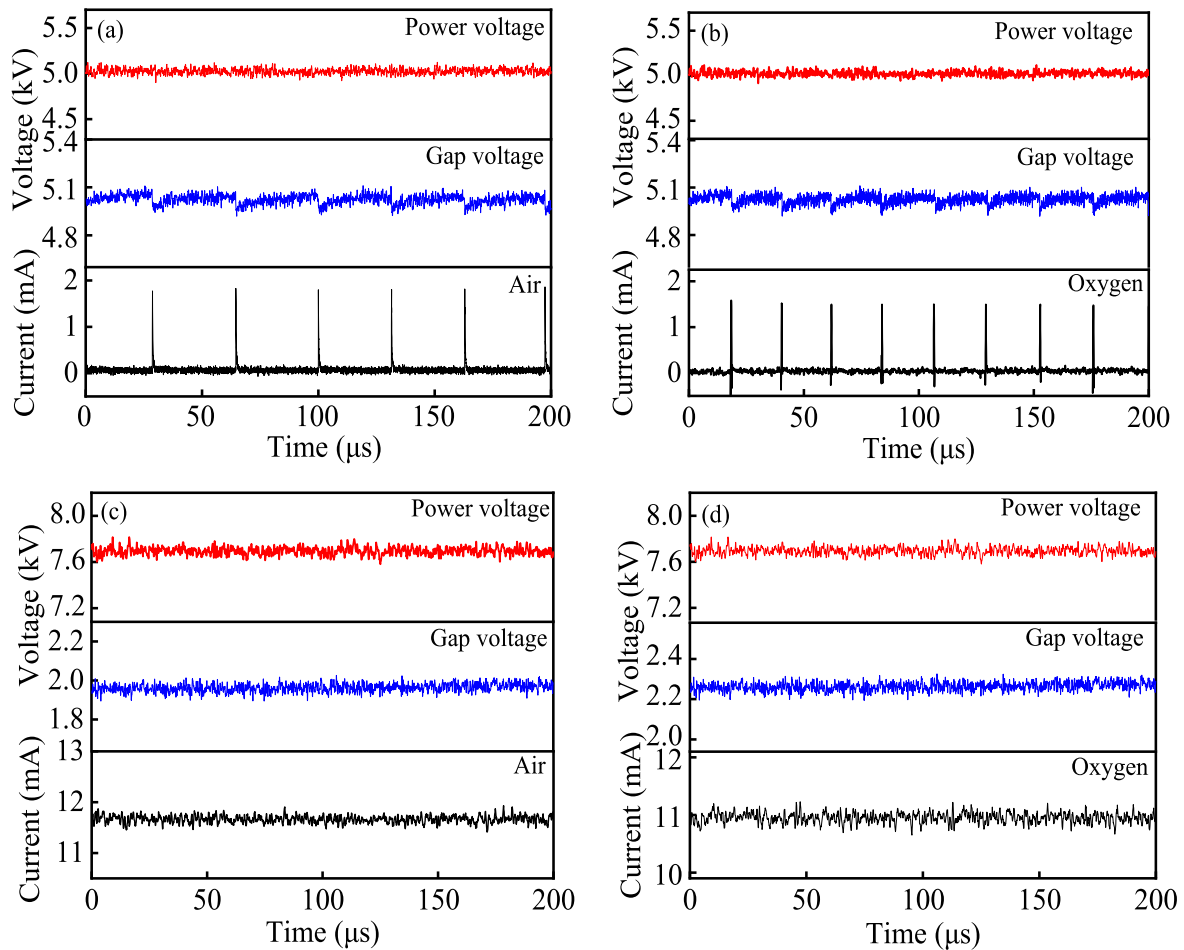
Figure 3. Waveforms of power voltage, gap voltage and discharge current. (a) to (d) correspond to figures 2(a) to (d), respectively.
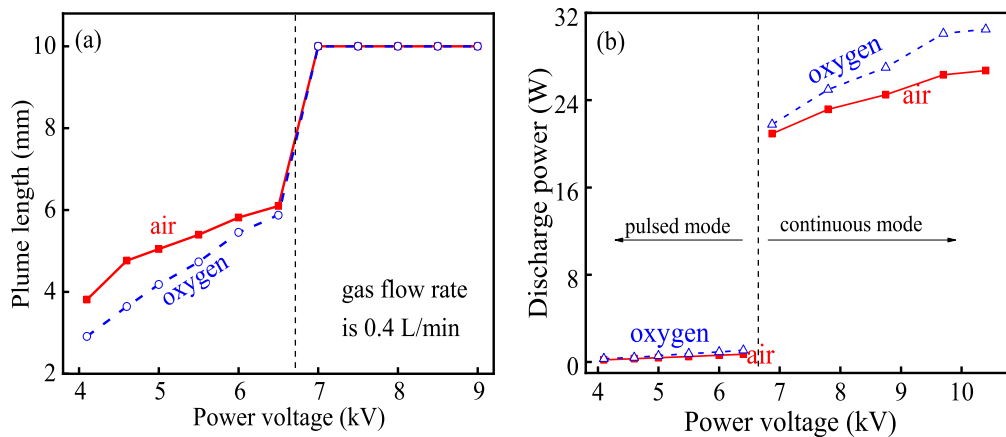

**Figure 4.** Plume length (a) and dissipated power (b) as functions of power voltage.

For the continuous mode, gap voltage and power voltage are investigated as functions of discharge current, as shown in figure 5(b). It reveals that power voltage increases, while gap voltage decreases with the increasing discharge current. As pointed out in [18], the negative slope of voltage-current curve suggests that the discharge operates in a normal glow discharge regime. Hence, the continuous mode in both gases belongs to a normal glow discharge regime. Besides, both gap and power voltages of oxygen discharge are higher than those

of air discharge under the same current, which also results from the electronegative nature of the oxygen molecule.

After 10 min treatment, degradation efficiency of MB with an initial concentration of $7.0\,mg\,l^{-1}$ is investigated as a function of power voltage in figure 6(a). Degradation efficiency for oxygen discharge increases with increasing power voltage. There is an abrupt decrement during the mode transition. Consequently, the pulsed oxygen discharge with power voltage of about 6.5 kV has the highest efficiency in
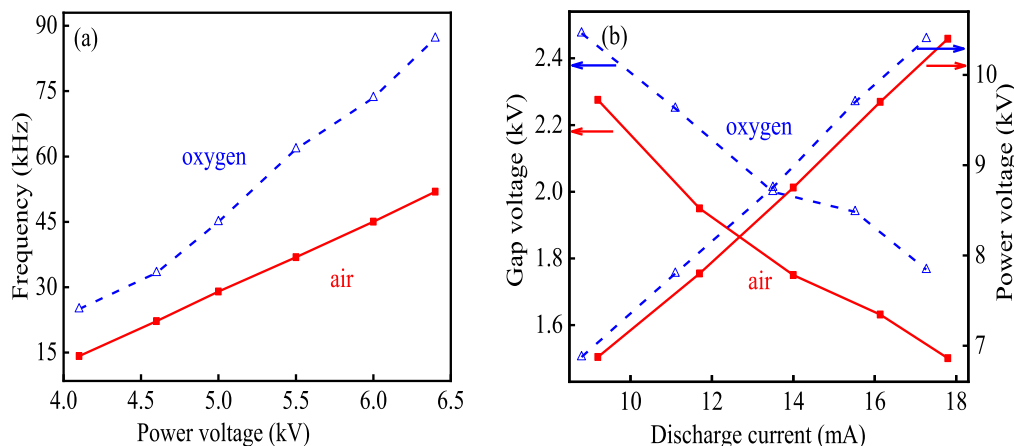
Figure 5. (a) Discharge frequency as a function of power voltage in the pulsed mode. (b) Characteristic of voltage and current in the continuous mode.
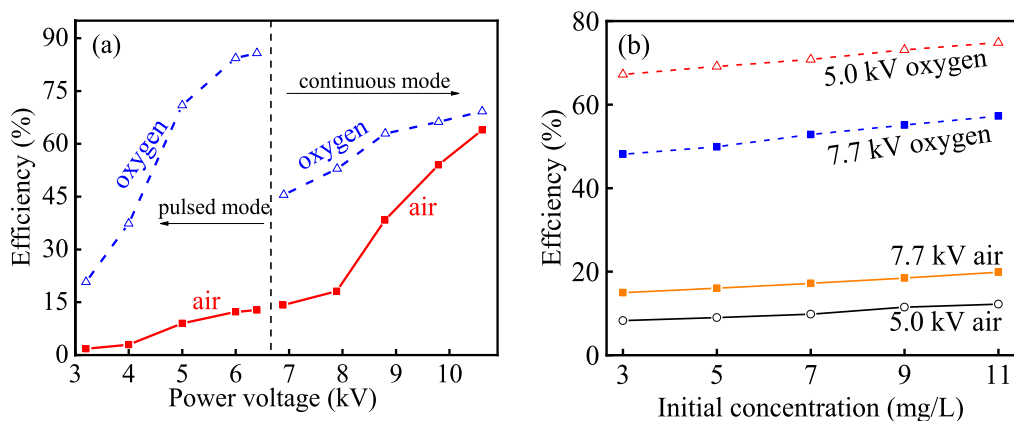
Figure 6. After 10 min treatment in air and oxygen discharges, degradation efficiency of MB dye as a function of power voltage (a) and initial solution concentration (b).

degrading MB dye, reaching approximately 85.8%. However, it monotonously increases with increasing power voltage for air discharge. Hence, a highest efficiency of 63.7% is obtained in the continuous mode at a power voltage of 10.6 kV. In contrast to air discharge under the same power voltage, oxygen discharge has a higher degradation efficiency. Figure 6(b) presents degradation efficiency of MB dye as a function of initial concentration of MB solution. It can be found that after 10 min treatment in air or oxygen discharge, MB degradation efficiency slightly increases with increasing initial concentration of MB solution. Moreover, oxygen discharge has a much higher degradation efficiency as compared to air discharge under the same power voltage and treatment time. Here, our measured results are not consistent with those reported by others [19].

Electron density in the pulsed mode is in the order of 10^{14}–10^{15} cm^{-3} [20], which is much higher than that of the glow discharge, typically 10^{12} cm^{-3} [21]. High electron density can produce more active species through electron collisions with neutral particle. Hence, degradation efficiency for oxygen discharge is higher in the pulsed mode than the continuous mode, even if the pulsed mode has a low voltage, such as 5.0 kV compared to 7.7 kV. Moreover, pulse frequency increases with increasing power voltage, which

implies that more oxygen atoms are produced per unit time. Hence, more MB dye is degraded per unit time, leading to a higher degradation efficiency (after 10 min treatment) with increasing power voltage. As a result, the highest efficiency of MB degradation is obtained at a voltage of 6.5 kV in the pulsed oxygen discharge before it transits to the continuous mode.

Optical spectra from the discharges are illustrated in the range from 200 nm to 900 nm in figure 7. For the pulsed air discharge, emission spectrum mainly consists of the second positive system of $N_2(C^3\Pi_u \rightarrow B^3\Pi_g)$, the system of $N_2(B^3\Pi_g \rightarrow A^3\Sigma_u)$, and the system of OH $(A^2\Sigma^+ \rightarrow X^2\Pi)$. Besides these systems, the spectral lines of O I (777 nm and 844 nm) can also be discerned. However, O I (777 nm and 844 nm) has very weak intensity in the pulsed air discharge. In fact, the system of OH appears at not only around 309 nm, but also 618 nm, which is the second diffraction of 309 nm. A typical OH spectrum peaked at 309 nm is presented in figure 7(b).

Active species (OH radical and oxygen atom) have high oxidation capability, which can effectively degrade MB dye through destructing C–C, C–H, C–N, C–O, N–H bonds and so on [22, 23]. The intensities of spectral lines (OH at 309 nm and O I at 777 nm) are investigated as functions of power
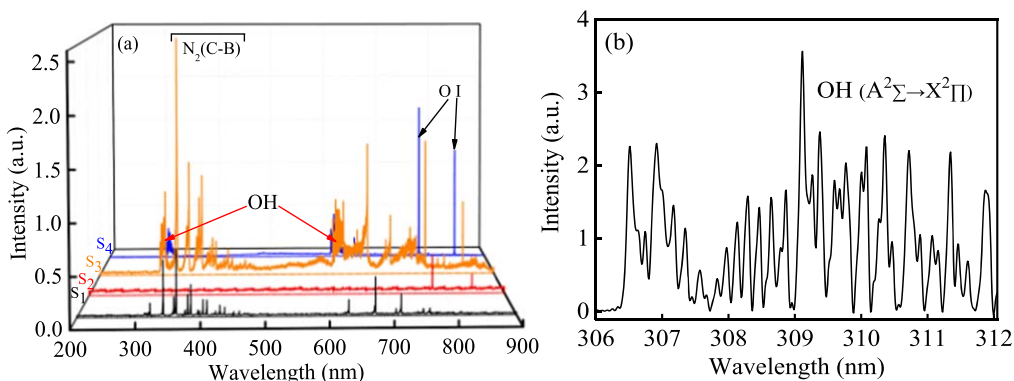
Figure 7. (a) 200 nm to 900 nm scanned emission spectra under different modes, among which S$_1$ to S$_4$ correspond to figures 2(a) to (d), respectively. (b) Detailed spectra of OH radical in oxygen discharge under a power voltage of 7.7 kV.
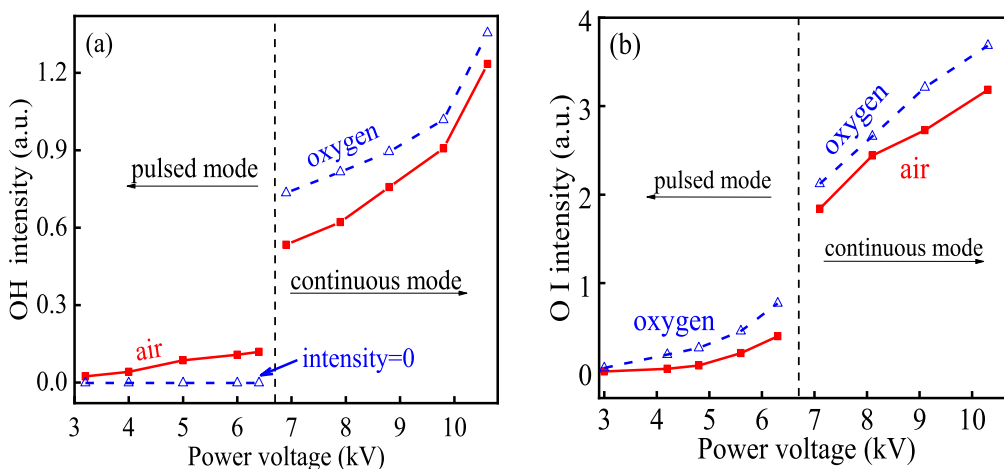

Figure 8. Emission intensities of OH peaked at 309 nm (a) and O I at 777.4 nm (b) as functions of power voltage.

voltage for air and oxygen discharges in figure 8. For the pulsed air discharge or the continuous mode in air or oxygen, spectral intensity of OH increases with increasing power voltage. An abrupt increment appears at the mode transition. In contrast to air discharge, spectral intensity of OH is hardly detectable for the pulsed oxygen discharge. However, for the continuous mode, it is higher in oxygen discharge than that in air discharge under the same power voltage. Besides, O I intensity increases with increasing power voltage for the discharge in air or oxygen, and an abrupt increment appears during the mode transition. Moreover, oxygen discharge has higher O I intensity as compared to air discharge with the same power voltage.

As mentioned before, plasma plume of the pulsed mode is normally shorter than the electrode separation of 10 mm, hence the plasma plume cannot directly touch the mesh, neither do the solution outside the mesh. Hence, we think the influence of the outside water on the discharge can be neglected. Because of lack of water vapor in oxygen, OH emission can hardly be detected in the pulsed oxygen discharge. However, being introduced into the plasma jet by an air compressor, trace vapor exists in air, which leads to a detectable spectral intensity of OH radical. Consequently, for the pulsed mode, spectral intensity of OH for oxygen discharge is lower than that for air discharge under the same

power voltage. For the continuous mode, gas temperature is much higher than that of the pulsed discharge [24], leading to a large amount of water being vaporized into the discharge zone. Hence, the abrupt increment of OH emission intensity appears during the mode transition.

As mentioned in the experimental setup, the CCD exposure time is kept constant at 0.5 s to investigate spectral intensities of OH and O I, which therein shows a temporally averaged result. Hence, it is meaningless to compare the intensities of the different modes. However, it is valuable to compare them in the same mode. For the continuous mode, they are higher in oxygen discharge than those in air discharge under the same power voltage. Hence, more OH radicals and oxygen atoms are generated per unit time in oxygen discharge than those in air discharge. As a result, oxygen discharge has higher degradation efficiency than air discharge. Based on the same reason, it can be inferred that for the pulsed mode, more oxygen atoms and less OH radicals are produced per unit time in oxygen discharge than those in air discharge. In combination with the higher MB degradation efficiency of the pulsed oxygen discharge than the pulsed air discharge, we can draw the conclusion that oxygen atoms play a more important role than OH radicals in MB degradation.
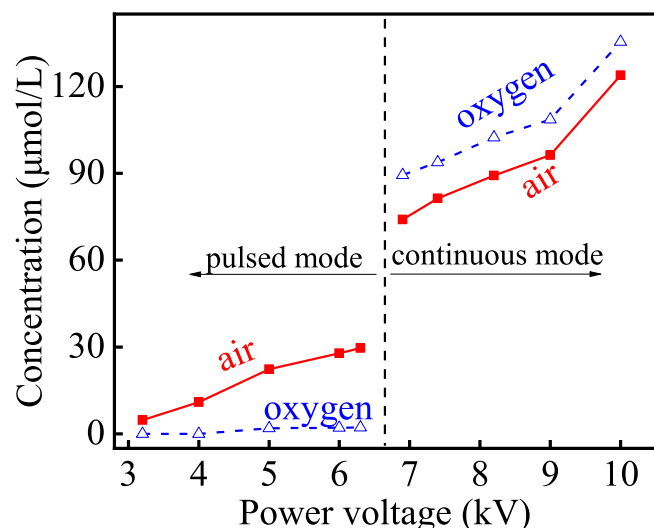
Figure 9. After ten minutes treatment of distilled water in air and oxygen discharges, the concentration of hydrogen peroxide as a function of power voltage.

Through using a colorimetric method [25, 26], H_2O_2 concentration as a function of power voltage is investigated, as shown in figure 9. It can be found that H_2O_2 concentration is very low in the pulsed oxygen discharge, while increases with increasing power voltage for the pulsed air discharge or the continuous mode in air or oxygen. Moreover, for the pulsed mode, hydrogen peroxide concentration in air discharge is higher than that in oxygen discharge under the same power voltage. However, it is reverse for the continuous mode. This result is consistent with that shown in figure 8, because hydrogen peroxide in solution mainly comes from recombination of OH radicals produced by the plasma jet.

Deionized water (3.4 μS/cm) and MB dye are used to obtain MB solution, which has an initial conductivity of 10.7 μS/cm. Initial conductivity is adjusted to 100 μS/cm by adding NaCl into MB solution to be treated. No obvious influence on the mode transition and the MB degradation can be observed. This can be attributed to the fact that solution is not introduced into the discharge circuit. In fact, oxygen atoms and OH radicals are brought into MB solution with the flowing gas, which then react with MB dye in the solution.

4. Conclusion

In summary, an underwater plasma jet excited by a DC voltage is employed to degrade MB dye by blowing air and oxygen in to MB solution. Discharge images reveal that the discharges only appear in the vicinity of the needle tip under a low power voltage, which is purple in air. It bridges the two electrodes under a high voltage, which is pink in air. Its morphology in oxygen discharge is similar to that in air discharge except that oxygen discharge is always white. Electrical aspects indicate that the discharge exhibits a pulsed mode and a continuous mode under different power voltages. For the pulsed mode, discharge frequency and plume length

are compared between air discharge and oxygen discharge, both of which increase with increasing power voltage. Moreover, air discharge has a longer plume and a lower pulse frequency. For the continuous mode, oxygen discharge has a higher power voltage and a higher gap voltage compared with air discharge under the same discharge current. Furthermore, the degradation efficiency of MB dye increases with increasing power voltage for either the pulsed mode or the continuous mode. The highest efficiency of about 85.8% is reached at about 6.5 kV in oxygen discharge. As a comparison, after 10 min treatment in air discharge, the highest degradation efficiency is 63.7%, which appears in the continuous mode at a power voltage of 10.6 kV. Compared with air discharge under the same power voltage, MB degradation efficiency is higher in oxygen discharge. Moreover, it increases with increasing initial concentration of MB solution. Optical emission spectra are also compared for the discharges in air and oxygen. Through investigating the spectral intensity of OH and O I, it is revealed that oxygen atoms play a more important role than OH radicals in MB degradation.

References

[1] Martínez-Huitle C A and Brillas E 2009 *Appl. Catal. B: Environ.* **87** 105
[2] Foster J *et al* 2012 *IEEE Trans. Plasma Sci.* **40** 1311
[3] Alhamedi F H, Rauf M A and Ashraf S S 2009 *Desalination* **239** 159
[4] Dong Y C *et al* 2007 *Dyes Pigm.* **73** 261
[5] Ji F *et al* 2011 *Desalination* **269** 284
[6] Lu N *et al* 2015 *IEEE Trans. Plasma Sci.* **43** 580
[7] Li X C *et al* 2018 *Plasma Process. Polym.* **15** 1700224
[8] Li X C *et al* 2019 *Plasma Sources Sci. Technol.* **28** 055006
[9] Lu X *et al* 2016 *Phys. Rep.* **630** 1
[10] Zhou X F *et al* 2019 *Plasma Process. Polym.* **16** 1800124
[11] Takemura Y, Yamaguchi N and Hara T 2013 *Jpn. J. Appl. Phys.* **52** 056102
[12] EL-Tayeb A *et al* 2016 *Contrib. Plasma Phys.* **56** 855
[13] Wang B W *et al* 2017 *Chem. Eng. Sci.* **168** 90
[14] Lu D L *et al* 2010 *IEEE Trans. Plasma Sci.* **38** 2854
[15] Foster J *et al* 2011 *Plasma Sources Sci. Technol.* **20** 034018
[16] Li X C *et al* 2017 *Plasma Sci. Technol.* **19** 115505
[17] Wu S Q *et al* 2018 *Phys. Plasmas.* **25** 123507
[18] Tang J *et al* 2012 *Phys. Plasmas.* **19** 013501

[19] Wu L H *et al* 2019 *Water* **11** 1818
[20] Wang X X *et al* 2018 *Plasma Sources Sci. Technol.* **27** 07LT02
[21] Raizer Y P 1991 *Gas Discharge Physics* (Berlin: Springer)
[22] Parkansky N *et al* 2012 *Plasma Chem. Plasma Process.* **32** 933
[23] Zaharie-Butucel D and Anghel S D 2014 *Rom. Journ. Phys.* **59** 757 (www.nipne.ro/rjp/2014_59_7-8/0757_0766.pdf)
[24] Xian Y B *et al* 2013 *Plasma Process. Polym.* **10** 372
[25] Eisenberg G 1943 *Ind. Eng. Chem. Anal. Ed.* **15** 327
[26] Li X C 2019 *Phys. Plasmas* **26** 033507